ELSEVIER

Inorganica Chimica Acta 228 (1995) 93–101

Inorganica Chimica Acta

Syntheses, structures and properties of copper and nickel complexes of the macrocyclic ligand 5,6,11,12,17,18,23,24-octahydro-tetrabenzo[*b,f,j,n*][1,5,9,13]tetraazacyclohexadecine (H_8TAAB)

Siegfried Schindler [1], David J. Szalda [2]

Chemistry Department, Brookhaven National Laboratory, Upton, NY 11973-5000, USA

Received 20 April 1994

Abstract

The synthesis and characterization of the new macrocyclic copper complex $[Cu(H_8TAAB](ClO_4)_2$ are described (H_8TAAB = 5,6,11,12,17,18,23,24-octahydro-tetrabenzo[*b,f,j,n*][1,5,9,13]tetraazacyclohexadecine). The crystal structure of the complex ($[Cu(H_8TAAB)(H_2O)_2](ClO_4)_2 \cdot 2H_2O$) was determined. Crystal data: formula $CuN_4C_{28}H_{36}Cl_2O_{12}$, space group $P\bar{1}$, $Z=2$, $a=9.475(2)$, $b=9.457(1)$, $c=18.222(4)$ Å, $\alpha=90.07(2)$, $\beta=97.71(2)$, $\gamma=90.02(1)°$. The nickel complex of H_8TAAB ($[Ni(H_8TAAB)(O(H)CH_3)_2](ClO_4)_2 \cdot 2HOCH_3$) crystallizes in the space group $P\bar{1}$; formula $NiN_4C_{32}H_{44}Cl_2O_{12}$, $Z=2$, $a=11.322(5)$, $b=16.752(9)$, $c=9.703(3)$ Å, $\alpha=101.24(4)$, $\beta=90.76(3)$, $\gamma=86.74(4)°$. For the ligand H_8TAAB which crystallized with one ethylacetate, formula $N_4C_{32}H_{36}O_2$, the space group $P2_1/c$ was found with $Z=4$, $a=18.468(3)$, $b=13.111(1)$, $c=11.698(2)$ Å, $\beta=96.36(1)°$. A new macrocycle, Me_4H_4TAAB, was synthesized by methylation of H_8TAAB and structurally characterized: formula $N_4C_{32}H_{36}$, space group $P\bar{1}$ with $Z=2$, $a=12.150(1)$, $b=12.344(2)$, $c=9.324(1)$ Å, $\alpha=90.642(9)$, $\beta=102.186(9)$, $\gamma=102.804(9)°$.

Keywords: Crystal structures; Copper complexes; Nickel complexes; Azamacrocycle complexes; Electrochemistry

1. Introduction

In our attempts to find transition metal complexes which are able to bind and activate carbon dioxide [1] we reinvestigated the chemistry of a series of macrocyclic metal complexes. While we were not successful in finding new carbon dioxide binding complexes we gained more insight into 16-membered macrocyclic complexes. Condensation of *o*-aminobenzaldehyde in the presence of metal ions leads to the formation of metal complexes with the macrocyclic ligands tribenzo[*b,f,j*][1,5,9]-triazacycloduodecine (TRI) and tetrabenzo[*b,f,j,n*]-[1,5,9,13]-tetraazacyclohexadecine (TAAB) [2,3]. Busch and co-workers extensively investigated the metal complexes of these ligands which do not exist in their free form [2–10]. Reduction of the nickel complex of TAAB leads to the nickel complex of the fully saturated macrocycle 5,6,11,12,17,18,23,24-octahydrotetrabenzo-[*b,f,j,n*][1,5,9,13]tetraazacyclohexadecine (H_8TAAB) [11]. In contrast to TAAB this macrocycle is stable in its free form. The nickel complex of H_8TAAB was investigated by Busch and co-workers, and the synthesis of the free ligand was described [11,12].

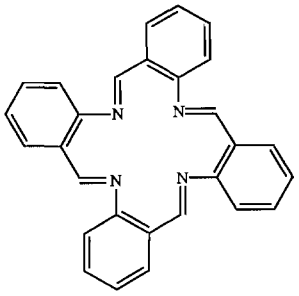

TAAB

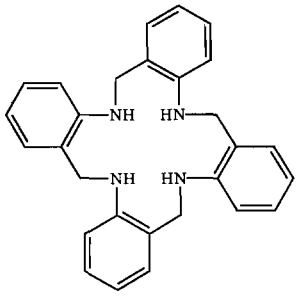

H_8TAAB

[1] Permanent address: Institute for Inorganic Chemistry, University of Witten-Herdecke, Stockhumer Strasse 10, 58448 Witten, Germany.

[2] Permanent address: Department of Natural Sciences, Baruch College, Manhattan, NY 10010, USA. Address questions concerning the X-ray crystallographic determinations to this author.

Elsevier Science S.A.
SSDI 0020-1693(94)04180-4

To our knowledge no further work on this interesting macrocycle has been reported. While reinvestigating these macrocyclic ligands we were able to synthesize and characterize the previously unknown copper(II) complex of H_8TAAB and succeeded in obtaining crystals of the free ligand and the nickel(II) complex suitable for X-ray structure determination. In addition we synthesized and crystallized the methylated form of this ligand but have so far been unable to obtain crystals of metal complexes of this ligand.

2. Experimental

2.1. Materials and methods

Reagents and solvents used were of commercially available reagent grade quality. UV–Vis spectra were measured in 1 cm quartz cells with $(0.5–10)\times10^{-4}$ M solutions on a Hewlett Packard 8452 A spectrophotometer. ^{1}H NMR spectra were recorded on a Bruker AM-300 300-MHz spectrometer. IR spectra were determined on a Mattson Polaris FT-IR spectrometer. Elemental analyses were performed by E. Norton, Brookhaven National Laboratory. H_8TAAB was prepared according to the published method [12].

2.1.1. $[Ni(H_8TAAB)(O(H)CH_3)_2](ClO_4)_2\cdot 2HOCH_3$

This was prepared by dissolving 100 mg (0.24 mMol) of H_8TAAB in 30 ml chloroform and a solution of 180 mg (0.5 mMol) of $Ni(ClO_4)_2\cdot 6H_2O$ in 20 ml methanol was added. The solution was kept for three weeks at −5 °C and some tiny pale green crystals formed which were suitable for X-ray analysis.

2.1.2. $[Cu(H_8TAAB)(H_2O)_2](ClO_4)_2\cdot 2H_2O$

This was synthesized by mixing a suspension of 100 mg (0.24 mMol) of H_8TAAB in 30 ml methanol with a solution of 185 mg (0.5 mMol) of $Cu(ClO_4)_2\cdot 6H_2O$ in 10 ml methanol. The solution turned green while the ligand H_8TAAB dissolved and 30 ml water were added. The solution was evaporated on a rotary evaporator at room temperature to ~35 ml and filtered. The solution in an open beaker was left on the lab bench for two days and green crystals formed which were filtered off and air dried. *Anal.* Calc. for $[CuH_8TAAB](ClO_4)_2\cdot 4H_2O$: Cu, 8.4; ClO_4, 26.3. Found: Cu, 8.6; ClO_4, 26.0%.

In addition it was possible to obtain this complex by reduction of the copper(II) complex of TAAB with sodium borohydride in acetonitrile. The solution turned to a deep red color and dilute perchloric acid was added after two minutes until the pH reached 5 (measured with wet pH paper). The solution turned green during the neutralization. Water was added and the acetonitrile evaporated. The residue was put on an ion exchange column (sephadex) and the complex was washed out with 0.5 M sodium perchlorate. Leaving the solution in an open beaker led to the formation of small green crystals after several days which are identical with the ones described above. This method also offers an alternative way to obtain the free ligand H_8TAAB. Without doing the ion exchange the solution above was treated with concentrated ammonia and extracted with chloroform. Reducing the volume of the chloroform solution and adding methanol led to H_8TAAB after a few days at −5 °C.

2.1.3. Me_4H_4TAAB

This was synthesized by reductive methylation of H_8TAAB according to published methods [13,14] with a slight modification of the general procedure. 100 mg (0.24 mMol) of H_8TAAB were dissolved in 30 ml chloroform, and acetonitrile was added until the solution became slightly cloudy. Formaldehyde (6 ml) was added, followed by 1 g of solid sodium cyanoborohydride. Concentrated acetic acid was slowly added to the stirred solution until the pH reached 6 (tested on wet pH paper). After stirring for ~1 h the progress of the reaction was checked by thin layer chromatography (solvent: hexane/ethylacetate, 10/1). If more than one spot was obtained, addition of formaldehyde, sodium cyanoborohydride and acetic acid was repeated. The resulting final suspension was evaporated to a paste on a rotary evaporator and after treatment with 4 M sodium hydroxide it was extracted with chloroform. The chloroform solution was dried over sodium sulfate and then evaporated to 10 ml and 30 ml of methanol were added. White crystals which were suitable for X-ray analysis formed when the solution was left for one week at −5 °C. ^{1}H NMR ($CDCl_3$): δ 2.63 (12H (methyl), s), 4.2 (8H (CH_2), broad), 6.8–7.5 (16H, (benzene), m).

2.2. Electrochemistry

Cyclic voltammetry (CV) and differential-pulse voltammetry (DPV) were performed with a BAS 100 instrument at 22±2 °C with (CV) a scan rate of 100 mV s^{-1} and (DPV) pulse height of 50 mV and a scan rate of 4 mV s^{-1}. The solutions studied contained 1 mM copper complex and 0.1 M tetrapropylammonium perchlorate in acetonitrile. A conventional H-type cell was used with glassy carbon, Pt and SCE as working, counter and reference electrodes, respectively. Ferrocene was used as an internal standard.

2.3. Collection and reduction of X-ray data

Crystals of $H_6TAAB \cdot CH_3CH_2OC(O)CH_3$ (**I**) were white prisms. A crystal $0.40 \times 0.50 \times 0.70$ mm was coated with petroleum jelly and mounted in a glass capillary tube. The diffraction data indicated the crystal to be monoclinic with systematic absences $0k0$, $k = 2n + 1$ and $h0l$, $l = 2n + 1$ consistent with space group $P2_1/c$ [15a].

Crystals of $[Ni(H_8TAAB)(O(H)CH_3)_2](ClO_4)_2 \cdot 2HOCH_3$ (**II**) were very light green prisms. A crystal $0.20 \times 0.30 \times 0.70$ mm was coated with petroleum jelly and placed in a capillary tube. The diffraction data indicated triclinic symmetry and space group $P\bar{1}$ [15b] was assumed for the solution and refinement of the crystal structure.

Crystals of $[Cu(H_8TAAB)(H_2O)_2](ClO_4)_2 \cdot 2H_2O$ (**III**) suitable for X-ray analysis were green prisms. A crystal $0.11 \times 0.22 \times 0.07$ mm was used for data collection. The crystal was mounted on a glass fiber. A triclinic unit cell was obtained by centering 19 reflections on a CAD-4 diffractometer. The CAD-4 software [16] suggested the presence of a primitive monoclinic cell. A survey of several reflections indicated that the reflections in this cell did not have monoclinic symmetry so a sphere of data to a value of $2\theta = 20°$ was collected to check for higher symmetry. Only triclinic symmetry was observed in the diffraction data so space group $P\bar{1}$ [15b] was assumed for the solution and refinement of the crystal structure. (Averaging the absorption corrected data assuming monoclinic symmetry results in an R_{av} of over 0.20.)

Crystals of Me_4H_4TAAB (**IV**) were colorless prisms and a crystal $0.55 \times 0.60 \times 0.65$ mm was cut from a larger crystal and mounted on a glass fiber. The diffraction data indicated triclinic symmetry and space group $P\bar{1}$ [15b] was assumed for the solution and refinement of the structure.

Crystal data and information on data collection for all four structures are given in Table 1; see also Section 5, Table S1.

2.4. Determination and refinement of structures

The structures of **II** and **III** were solved by standard Patterson heavy-atom methods while the structures of **I** and **IV** were solved by direct methods [17]. In the full-matrix (refined in two blocks) least-squares refinement [17], neutral-atom scattering factors [18] and corrections for anomalous dispersion were used and the quantity $\Sigma w(|F_o| - |F_c|)^2$ was minimized. Anisotropic temperature parameters were used for all the non-hydrogen atoms (except for the two carbons in the partial occupancy ethyl group in **I**). For **II** and **III** during the final cycles of refinement, hydrogen atoms were introduced in their calculated positions (X–H = 0.95 Å) and allowed to 'ride' [17] on the C or N atom to which they were bound. A common isotropic thermal parameter was refined for all of the hydrogens in **II** and **III**. The hydrogen atoms in **I** and **IV** were found on difference Fourier maps and their positional and individual isotropic thermal parameters were refined (excepted for the hydrogens on the ethylacetate in **I** which were placed in calculated positions and treated

Table 1
Crystallographic data for $H_8TAAB \cdot CH_3CH_2OC(O)CH_3$ (**I**), $[Ni(H_8TAAB)(O(H)CH_3)_2](ClO_4)_2 \cdot 2HOCH_3$ (**II**), $[Cu(H_8TAAB)(H_2O)_2](ClO_4)_2 \cdot 2H_2O$ (**III**) and Me_4H_4TAAB (**IV**)

Formula	$N_4C_{32}H_{36}O_2$	$NiN_4C_{32}H_{44}Cl_2O_{12}$	$CuN_4C_{28}H_{36}Cl_2O_{12}$	$N_4C_{32}H_{36}$
a (Å)	18.468(3)	11.322(5)	9.475(2)	12.150(1)
b (Å)	13.111(1)	16.752(9)	9.457(1)	12.344(2)
c (Å)	11.698(2)	9.703(3)	18.222(4)	9.324(1)
α (°)		101.24(4)	90.07(2)	90.642(9)
β (°)	96.36(1)	90.76(3)	97.71(2)	102.186(9)
γ (°)		86.74(4)	90.02(1)	102.804(9)
V (Å^3)	2815.4(7)	1802(1)	1618.0(5)	1330.4(3)
Z	4	2	2	2
FW	508.66	806.99	755.06	476.66
Space group	$P2_1/c$	$P\bar{1}$	$P\bar{1}$	$P\bar{1}$
ρ_{calc} (g cm^{-3})	1.200	1.487	1.550	1.190
λ (graphite monochromatized) (Å)	1.5418 (Cu Kα)	0.71069 (Mo Kα)	0.71069 (Mo Kα)	0.71069 (Mo Kα)
μ (cm^{-1})	6.1	7.6	9.38	0.762
Transmission coefficient	0.529–0.838	0.614–0.876	0.890–0.938	
R^a	0.053	0.086	0.076	0.045
$R_w{}^a$	0.078	0.089	0.051	0.060
Max. shift/error final cycle	≤ 0.01	≤ 0.02	≤ 0.05	≤ 0.01
T (K)	295	294	295	295

[a] $R = \Sigma||F_o| - |F_c||/\Sigma|F_o|$; $R_w = \{\Sigma[w(|F_o| - |F_c|)^2]/\Sigma w|F_o|^2]\}^{1/2}$.

like the hydrogens in II and III.) The atomic coordinates for the non-hydrogen atoms are listed in Tables 2–5.

3. Results

3.1. Syntheses

The synthesis of H_8TAAB according to the literature [12] was straightforward and led to a slightly yellow powder. One synthesis led to white crystals which proved to be H_8TAAB by crystallography but with a 20% impurity of an ethyl derivative. Synthesis of the nickel complex of H_8TAAB was difficult and many times the ligand came out of the solvent mixtures without forming the complex. Only very few crystals were obtained in the described procedure. In contrast synthesis of the copper complex of H_8TAAB was easy. Preparation of

Table 2
Positional parameters[a] for the non-hydrogen atoms in $H_8TAAB \cdot CH_3CH_2OC(O)CH_3$ (I)

Atom	x	y	z	U_{eq}[c]
N1	0.83107(16)	0.4683(2)	0.5091(2)	0.059
C1	0.8905(2)	0.4091(3)	0.4699(3)	0.061
C11	0.87987(18)	0.3904(3)	0.3416(3)	0.055
C12	0.82186(18)	0.3302(2)	0.2925(3)	0.052
C13	0.8159(2)	0.3122(3)	0.1742(3)	0.065
C14	0.8655(3)	0.3512(3)	0.1079(4)	0.080
C15	0.9221(3)	0.4098(3)	0.1547(4)	0.080
C16	0.9298(2)	0.4289(3)	0.2735(3)	0.068
N2	0.77313(16)	0.2887(2)	0.3620(3)	0.061
C2	0.7124(2)	0.2266(4)	0.3146(4)	0.069
C21	0.66285(18)	0.1992(3)	0.4032(3)	0.063
C22	0.62126(18)	0.2736(3)	0.4502(3)	0.063
C23	0.5740(2)	0.2456(4)	0.5310(4)	0.075
C24	0.5683(2)	0.1437(4)	0.5618(4)	0.084
C25	0.6084(3)	0.0714(4)	0.5152(5)	0.091
C26	0.6558(2)	0.0992(3)	0.4367(4)	0.081
N3	0.62720(17)	0.3762(2)	0.4175(3)	0.074
C3	0.5659(2)	0.4426(3)	0.4188(5)	0.084
C31	0.5796(2)	0.5471(3)	0.3738(4)	0.073
C32	0.63389(19)	0.6101(3)	0.4305(3)	0.065
C33	0.6407(3)	0.7100(3)	0.3932(4)	0.079
C34	0.5969(3)	0.7464(4)	0.2990(5)	0.094
C35	0.5458(3)	0.6836(5)	0.2395(5)	0.103
C36	0.5368(3)	0.5852(4)	0.2779(4)	0.089
N4	0.67836(17)	0.5709(2)	0.5242(3)	0.075
C4'[b]	0.6702(11)	0.4689(15)	0.5423(18)	0.129
C4"[b]	0.6203(14)	0.4857(20)	0.641(2)	0.105
C4	0.7396(2)	0.6298(3)	0.5765(4)	0.064
C41	0.78828(19)	0.5683(3)	0.6621(3)	0.058
C42	0.83398(18)	0.4927(3)	0.6264(3)	0.054
C43	0.8808(2)	0.4399(3)	0.7088(3)	0.064
C44	0.8806(2)	0.4636(4)	0.8243(3)	0.075
C45	0.8362(3)	0.5375(4)	0.8595(4)	0.078
C46	0.7911(3)	0.5889(4)	0.7789(4)	0.072
C51	0.2552(2)	0.0771(3)	0.3150(4)	0.088
C52	0.1877(2)	0.1314(3)	0.2700(4)	0.070
O52	0.16584(19)	0.1427(2)	0.1695(3)	0.093
O53	0.15195(14)	0.1659(2)	0.3549(2)	0.072
C54	0.0817(2)	0.2146(3)	0.3221(4)	0.086
C55	0.0497(3)	0.2333(4)	0.4313(5)	0.120

[a] Numbers in parentheses are errors in the last significant digit(s).
[b] Atoms C4' and C4" have occupancy factors equal to 0.20.
[c] $U_{eq} = \frac{1}{3}\Sigma_i\Sigma_j U_{ij} a^*_i a^*_j \mathbf{a}_i \cdot \mathbf{a}_j$.

Table 3
Positional parameters[a] for the non-hydrogen atoms in $[Ni(H_8TAAB)(O(H)CH_3)_2](ClO_4)_2 \cdot 2HOCH_3$ (II)

Atom	x	y	z	U_{eq}[b]
Ni	0.22019(14)	0.25277(10)	0.45717(17)	0.037
N1	0.0446(8)	0.3020(6)	0.4322(10)	0.047
C1	0.0354(10)	0.3928(7)	0.4480(13)	0.049
C11	0.1173(10)	0.4172(7)	0.3426(13)	0.042
C12	0.2370(11)	0.4069(7)	0.3551(13)	0.042
C13	0.3108(11)	0.4270(8)	0.2530(16)	0.069
C14	0.2621(13)	0.4611(9)	0.1491(15)	0.071
C15	0.1424(13)	0.4723(8)	0.1373(14)	0.060
C16	0.0674(11)	0.4507(8)	0.2348(14)	0.057
N2	0.2855(8)	0.3703(6)	0.4683(10)	0.041
C2	0.4163(10)	0.3728(8)	0.4886(14)	0.060
C21	0.4526(10)	0.3437(9)	0.6189(14)	0.054
C22	0.4403(10)	0.2619(9)	0.6276(14)	0.050
C23	0.4726(11)	0.2348(9)	0.7498(16)	0.065
C24	0.5124(12)	0.2880(11)	0.8643(16)	0.076
C25	0.5227(12)	0.3658(11)	0.8599(16)	0.073
C26	0.4928(12)	0.3957(10)	0.7387(18)	0.070
N3	0.3941(8)	0.2097(6)	0.5042(10)	0.051
C3	0.4007(11)	0.1201(8)	0.5082(14)	0.056
C31	0.3566(12)	0.0702(8)	0.3748(14)	0.049
C32	0.2366(13)	0.0744(7)	0.3376(14)	0.053
C33	0.1991(12)	0.0279(8)	0.2132(15)	0.058
C34	0.2785(17)	−0.0235(9)	0.1274(16)	0.074
C35	0.3961(16)	−0.0279(9)	0.1663(19)	0.079
C36	0.4353(13)	0.0194(9)	0.2893(15)	0.060
N4	0.1590(9)	0.1320(6)	0.4286(10)	0.053
C4	0.0324(12)	0.1277(8)	0.3909(14)	0.060
C41	−0.0442(11)	0.1851(8)	0.4991(13)	0.053
C42	−0.0420(10)	0.2685(9)	0.5166(14)	0.053
C43	−0.1114(11)	0.3215(9)	0.6185(15)	0.066
C44	−0.1871(13)	0.2848(11)	0.6969(16)	0.077
C45	−0.1916(14)	0.2036(12)	0.6823(18)	0.092
C46	−0.1206(12)	0.1525(9)	0.5826(16)	0.078
O5	0.1841(7)	0.2688(5)	0.6759(9)	0.053
C5	0.1804(13)	0.3365(9)	0.7926(14)	0.079
O6	0.2354(8)	0.2296(5)	0.2351(9)	0.057
C6	0.3346(15)	0.2116(10)	0.1442(17)	0.104
O7	0.5992(13)	0.2180(9)	0.3235(19)	0.150
C7	0.663(2)	0.1714(14)	0.263(3)	0.196
O8	0.0256(20)	0.230(2)	0.103(2)	0.297
C8	−0.035(3)	0.223(2)	0.033(3)	0.256
Cl1	0.1810(4)	0.0594(3)	0.7900(4)	0.083
O11	0.1047(9)	0.0245(7)	0.8726(10)	0.127
O12	0.2938(10)	0.0553(9)	0.8356(13)	0.164
O13	0.1693(16)	0.0294(9)	0.6525(13)	0.238
O14	0.1521(15)	0.1419(8)	0.8038(16)	0.193
Cl2	0.7267(3)	0.4081(3)	0.2379(5)	0.081
O21	0.7940(11)	0.3423(8)	0.2647(15)	0.159
O22	0.7614(12)	0.4767(9)	0.3170(17)	0.160
O23	0.6104(10)	0.3935(8)	0.2157(14)	0.145
O24	0.7627(17)	0.4175(15)	0.1062(18)	0.306

[a] Numbers in parentheses are errors in the last significant digit(s).
[b] $U_{eq} = \frac{1}{3}\Sigma_i\Sigma_j U_{ij} a^*_i a^*_j \mathbf{a}_i \cdot \mathbf{a}_j$.

Table 4
Positional parameters [a] for the non-hydrogen atoms in $[Cu(H_8TAAB)(H_2O)_2](ClO_4)_2 \cdot 2H_2O$ (III)

Atom	x	y	z	U_{eq} [b]
Cu1	0.00643(9)	−0.07667(9)	−0.24973(5)	0.031
O5	−0.0474(5)	−0.0914(5)	−0.3818(3)	0.056
O6	0.0604(5)	−0.0825(5)	−0.1184(2)	0.050
N1	0.2259(5)	−0.0820(5)	−0.2477(3)	0.030
C1	0.2959(7)	0.0574(7)	−0.2366(4)	0.043
C11	0.2457(7)	0.1502(7)	−0.2999(4)	0.038
C12	0.1011(7)	0.1845(6)	−0.3156(4)	0.035
C13	0.0499(8)	0.2544(6)	−0.3809(4)	0.042
C14	0.1442(10)	0.2946(7)	−0.4286(4)	0.061
C15	0.2867(10)	0.2688(8)	−0.4122(5)	0.064
C16	0.3355(8)	0.1966(7)	−0.3490(4)	0.054
N2	0.0091(5)	0.1398(5)	−0.2628(3)	0.033
C2	−0.1375(7)	0.2045(7)	−0.2751(4)	0.042
C21	−0.2062(7)	0.1821(7)	−0.2062(4)	0.037
C22	−0.2322(6)	0.0476(7)	−0.1827(4)	0.035
C23	−0.2787(7)	0.0258(7)	−0.1145(4)	0.043
C24	−0.3031(8)	0.1417(9)	−0.0715(4)	0.056
C25	−0.2836(9)	0.2752(9)	−0.0960(5)	0.065
C26	−0.2357(7)	0.2965(7)	−0.1625(4)	0.055
N3	−0.2036(5)	−0.0692(5)	−0.2304(3)	0.033
C3	−0.2570(7)	−0.2103(6)	−0.2081(4)	0.040
C31	−0.2597(7)	−0.3112(6)	−0.2716(4)	0.036
C32	−0.1330(7)	−0.3459(6)	−0.2988(4)	0.033
C33	−0.1384(8)	−0.4234(6)	−0.3632(4)	0.042
C34	−0.2689(9)	−0.4704(7)	−0.3984(4)	0.055
C35	−0.3922(9)	−0.4423(8)	−0.3702(5)	0.065
C36	−0.3881(7)	−0.3613(7)	−0.3074(4)	0.047
N4	−0.0027(5)	−0.2959(5)	−0.2577(3)	0.033
C4	0.1306(7)	−0.3610(7)	−0.2797(4)	0.040
C41	0.2503(7)	−0.3325(7)	−0.2207(4)	0.036
C42	0.2921(7)	−0.1944(7)	−0.2012(3)	0.036
C43	0.3882(7)	−0.1683(8)	−0.1389(4)	0.047
C44	0.4487(8)	−0.2821(10)	−0.0973(4)	0.061
C45	0.4161(9)	−0.4154(11)	−0.1183(5)	0.070
C46	0.3168(8)	−0.4432(8)	−0.1788(5)	0.058
Cl1	−0.1791(2)	−0.25892(19)	0.05095(10)	0.052
O11	−0.1943(6)	−0.3824(5)	0.0056(3)	0.078
O12	−0.1237(5)	−0.2988(5)	0.1243(3)	0.066
O13	−0.3102(6)	−0.1900(7)	0.0511(3)	0.098
O14	−0.0800(6)	−0.1651(5)	0.0234(3)	0.084
Cl2	−0.2755(2)	0.1877(2)	0.45902(10)	0.051
O21	−0.3767(6)	0.1888(6)	0.5093(3)	0.081
O22	−0.2022(6)	0.3181(6)	0.4603(3)	0.087
O23	−0.1759(6)	0.0759(6)	0.4790(3)	0.079
O24	−0.3465(5)	0.1611(5)	0.3857(3)	0.065
OW1	0.0198(6)	−0.3831(6)	−0.0982(3)	0.084
OW2	−0.3558(5)	−0.0415(6)	−0.3851(3)	0.075

[a] Numbers in parentheses are errors in the last significant digit(s).
[b] $U_{eq} = \frac{1}{3}\Sigma_i\Sigma_j U_{ij} a^*_i a^*_j \mathbf{a}_i \cdot \mathbf{a}_j$.

Me_4H_4TAAB was time consuming and only small yields were obtained. No nickel or copper complexes of this new macrocycle could be obtained. While we observed a color change in the reaction of copper perchlorate with Me_4H_4TAAB in a chloroform/methanol mixture we only succeeded in recovering the ligand when we were trying to isolate the complex. Heating the solution led to decomposition.

Table 5
Positional parameters [a] for the non-hydrogen atoms in Me_4H_4TAAB (IV)

Atom	x	y	z	U_{eq} [b]
C17	0.5055(2)	0.3033(3)	0.3284(3)	0.079
N1	0.41040(12)	0.26899(11)	0.40399(15)	0.048
C1	0.41889(15)	0.16862(14)	0.48340(19)	0.047
C11	0.52533(14)	0.18027(13)	0.60509(18)	0.043
C12	0.53592(14)	0.23072(14)	0.74273(19)	0.046
C13	0.63322(16)	0.23119(18)	0.8525(2)	0.061
C14	0.71906(17)	0.1815(2)	0.8277(3)	0.069
C15	0.70891(17)	0.13141(17)	0.6918(3)	0.064
C16	0.61383(16)	0.13148(15)	0.5836(2)	0.053
C27	0.4895(2)	0.39885(19)	0.8207(4)	0.075
N2	0.44522(11)	0.28157(12)	0.77077(15)	0.047
C2	0.38112(16)	0.22032(16)	0.87411(19)	0.049
C21	0.30536(14)	0.10917(13)	0.81061(17)	0.044
C22	0.18676(14)	0.09534(12)	0.74602(16)	0.040
C23	0.12116(17)	−0.01164(14)	0.6967(2)	0.052
C24	0.17102(19)	−0.10237(16)	0.7087(2)	0.063
C25	0.2857(2)	−0.08960(17)	0.7697(3)	0.069
C26	0.35200(18)	0.01595(16)	0.8210(2)	0.059
C37	0.00850(16)	0.16170(17)	0.7190(2)	0.054
N3	0.13383(11)	0.18704(10)	0.73952(14)	0.042
C3	0.17456(16)	0.27660(13)	0.64830(19)	0.044
C31	0.17534(13)	0.39179(13)	0.70887(17)	0.041
C32	0.17808(13)	0.48276(13)	0.61830(18)	0.043
C33	0.17236(16)	0.58488(14)	0.6791(2)	0.052
C34	0.16630(17)	0.59767(16)	0.8232(2)	0.058
C35	0.16573(18)	0.51014(17)	0.9114(2)	0.060
C36	0.17079(16)	0.40839(15)	0.8547(2)	0.052
C47	0.1540(2)	0.55928(18)	0.3754(3)	0.066
N4	0.17929(12)	0.46963(11)	0.46807(14)	0.050
C4	0.27128(5)	0.42256(14)	0.43101(19)	0.047
C41	0.22696(14)	0.32390(13)	0.31945(16)	0.044
C42	0.29797(14)	0.25192(13)	0.30462(17)	0.045
C43	0.25741(17)	0.16223(15)	0.1999(2)	0.056
C44	0.14738(18)	0.14275(17)	0.1139(2)	0.058
C45	0.07612(17)	0.21134(17)	0.1306(2)	0.058
C46	0.11534(16)	0.30167(16)	0.23208(19)	0.055

[a] Numbers in parentheses are errors in the last significant digit(s).
[b] $U_{eq} = \frac{1}{3}\Sigma_i\Sigma_j U_{ij} a^*_i a^*_j \mathbf{a}_i \cdot \mathbf{a}_j$.

3.2. Structures

A view of the ligand, H_8TAAB, can be seen in Fig. 1. The atom labeling scheme used for the ligand in all four structures is also presented in this Figure. The crystal also contains an ethylacetate of crystallization. This ethylacetate is hydrogen bonded to one of the amine hydrogens of the ligand. The three other amine hydrogen form weak intramolecular hydrogen bonds with adjacent amines (see Table 6). The four nitrogen atoms of the ligand lie within ±0.13 Å of the least-squares plane defined by the four nitrogen atoms. The four hydrogen atoms on the nitrogen atoms of the ligand are alternately above and below the plane formed by the four nitrogens. Near the end of the refinement some extra electron density was observed around N(4). To account for this electron density, the presence of an impurity of about 20% of an ethyl substituted ligand

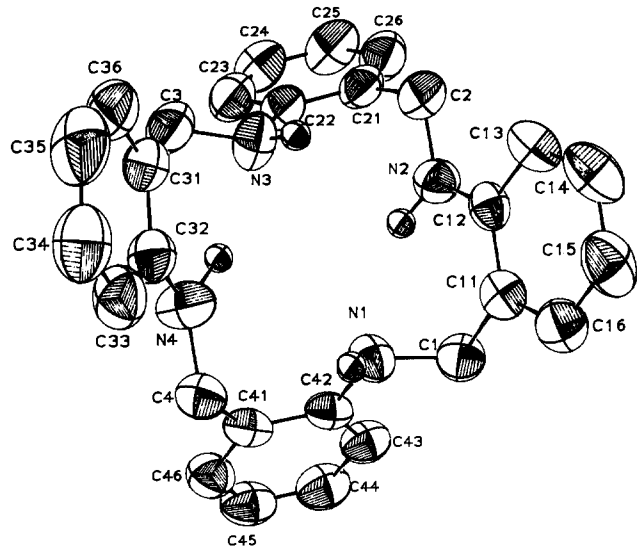

Fig. 1. An ORTEP drawing of $H_8TAAB \cdot CH_3CH_2OC(O)CH_3$ (I). The thermal ellipsoids are at the 50% probability level and the ethylacetate of crystallization and all the hydrogen atoms except for the amine hydrogens are omitted for clarity. The atom labeling scheme used for the ligand in all four structures is presented here.

Table 6
Proposed hydrogen bonding in $H_8TAAB \cdot CH_3CH_2OC(O)CH_3$ (I)

D–H···A	D–H (Å)	H···A (Å)	D···A (Å)	∠D–H···A (°)
N1–H1···O52[a]	1.02	2.14	3.10	156
N2–H2···N1	0.91	2.26	3.04	144
N3–H3···N2	1.01	2.52	3.06	114
N4–H4···N3	1.36	2.00	2.95	122

[a] $1-x, \frac{1}{2}+y, \frac{1}{2}-z$.

was assumed. This disorder was modeled by having H(4) 80% occupancy and C(4′) 20% occupancy share a site and C(4″) with a 20% occupancy factor represent the second carbon of the ethyl group. The introduction and refinement of this group satisfactorily accounted for the extra electron density. As a result of H(4) and C(4′) sharing a position the nitrogen hydrogen bond length is longer than normal while the nitrogen carbon bond length is shorter than normal. Selected bond lengths and angles are listed in Table 7.

A view of the cation $[Ni(H_8TAAB)(O(H)CH_3)_2]^{2+}$ can be seen in Fig. 2. The nickel(II) has an octahedral coordination sphere in which the four nitrogen atoms of the ligand form an equatorial plane with two methanols in the axial positions. The hydrogen atom on *trans* nitrogen atoms are on the same side of the ligand. This arrangement permits the benzene rings in the ligand adjacent to one another to be on opposite sides of the ligand resulting in the ligand having a saddle shape. All six metal to ligand bond lengths are approximately equal (average $Ni–N_{eq}$-2.135(10) Å and $Ni–O_{ax}$=2.126(9) Å, see Table 7). These are similar

Table 7
Selected bond distances (Å) and angles (°)[a] for $H_8TAAB \cdot CH_3CH_2OC(O)CH_3$ (I), $[Ni(H_8TAAB)(O(H)CH_3)_2](ClO_4)_2 \cdot 2HOCH_3$ (II), $[Cu(H_8TAAB)(H_2O)_2](ClO_4)_2 \cdot 2H_2O$ (III) and Me_4H_4TAAB (IV)

Bond distances (Å) in the metal coordination sphere in II and III

	II: X=Ni	III: X=Cu
X–N(1)	2.138(9)	2.076(5)
X–N(2)	2.125(10)	2.062(5)
X–N(3)	2.133(9)	2.068(5)
X–N(4)	2.142(11)	2.079(5)
X–O(5)	2.129(8)	2.395(5)
X–O(6)	2.122(9)	2.380(4)

Bond angles (°) in the metal coordination sphere in II and III

	II: X=Ni	III: X=Cu
N(1)–X–N(2)	89.7(4)	89.9(2)
N(1)–X–N(3)	174.1(4)	169.2(2)
N(1)–X–N(4)	91.1(4)	90.5(2)
N(1)–X–O(5)	87.6(3)	95.4(2)
N(1)–X–O(6)	87.7(3)	84.4(2)
N(2)–X–N(3)	88.6(4)	90.7(2)
N(2)–X–N(4)	175.4(4)	169.5(2)
N(2)–X–O(5)	95.3(3)	86.8(2)
N(2)–X–O(6)	90.2(3)	97.8(2)
N(3)–X–N(4)	91.0(4)	90.8(2)
N(3)–X–O(5)	87.0(3)	95.4(2)
N(3)–X–O(6)	98.0(4)	84.9(2)
N(4)–X–O(5)	89.3(4)	82.7(2)
N(4)–X–O(6)	85.3(4)	92.7(2)
O(5)–X–O(6)	172.7(3)	175.3(2)

Bond distances (Å) in ligand

	I	II	III	IV
C(42)–N(1)	1.403(4)	1.487(17)	1.450(8)	1.450(2)
N(1)–C(1)	1.459(5)	1.496(16)	1.479(8)	1.462(2)
C(12)–N(2)	1.389(5)	1.446(16)	1.446(9)	1.449(2)
N(2)–C(2)	1.445(5)	1.494(14)	1.507(8)	1.476(2)
C(22)–N(3)	1.407(5)	1.449(15)	1.452(8)	1.416(2)
N(3)–C(3)	1.430(5)	1.507(17)	1.503(8)	1.465(2)
C(32)–N(4)	1.392(5)	1.440(16)	1.435(8)	1.412(2)
N(4)–C(4)	1.447(5)	1.477(17)	1.507(8)	1.467(3)

to values found in high-spin nickel(II) complexes in which the nickel(II) is octahedrally coordinated [19,20] rather than those found in low-spin complexes in which the nickel is normally square planar. This is consistent with the magnetic measurements of Busch and coworkers [11] on $[Ni(H_8TAAB)]^{2+}$. The four nitrogen atoms of the ligand lie within ±0.10 Å of the least-squares plane formed by them. The nickel(II) ion lies in this plane. The two coordinated methanols are involved in strong hydrogen bonds.

A view of the cation $[Cu(H_8TAAB)(H_2O)_2]^{2+}$ is presented in Fig. 3. The metal coordination sphere is similar to that of the nickel complex except that the axial positions are occupied by water molecules and the metal coordination sphere exhibits the elongation of the axial bond lengths (av. $Cu–N_{eq}$=2.071(5) Å and

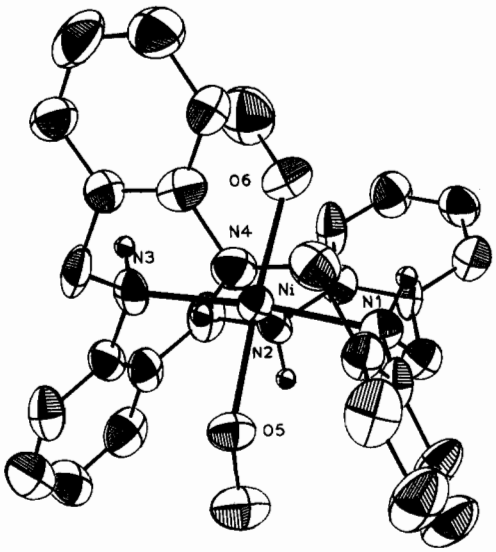

Fig. 2. An ORTEP drawing, with the thermal ellipsoids at the 50% probability level, of the cation of $Ni(H_8TAAB)(O(H)CH_3)_2](ClO_4)_2 \cdot 2HOCH_3$ (II). The axial coordination site of the metal center are occupied by two methanol molecules.

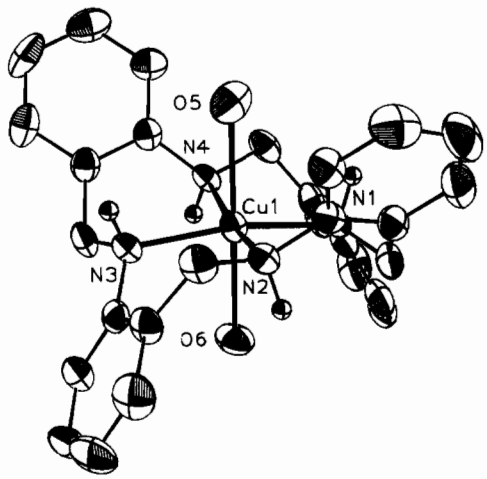

Fig. 3. An ORTEP drawing, with the thermal ellipsoids at the 50% probability level, of the cation of $[Cu(H_8TAAB)(H_2O)_2](ClO_4)_2 \cdot 2H_2O$ (III). Two water molecules are coordinated to the axial coordination sites of the copper(II) metal center.

av. $Cu-O_{ax} = 2.388(5)$ Å, see Table 7) which is typical for copper(II). The four nitrogen atoms of the ligand are within ± 0.19 Å of the least-squares plane formed by them. The copper(II) ion lies in this plane.

A view of the tetramethylated derivative of H_8TAAB, Me_4H_4TAAB, is presented in Fig. 4. The methylation of the amine nitrogen atoms forces the molecule to twist so that the four nitrogen atoms are no longer almost coplanar as was found for H_8TAAB but the ligand again is saddle shaped.

3.3. Spectral properties

The IR spectra of the copper complex of H_8TAAB showed the same characteristic frequencies as was found

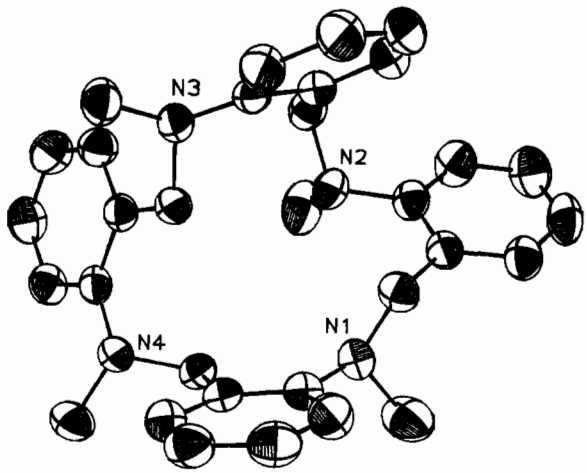

Fig. 4. An ORTEP view, with the thermal ellipsoids at the 50% probability level, of Me_4H_4TAAB (IV). The amine hydrogens of H_8TAAB (I) have been replaced by methyl groups.

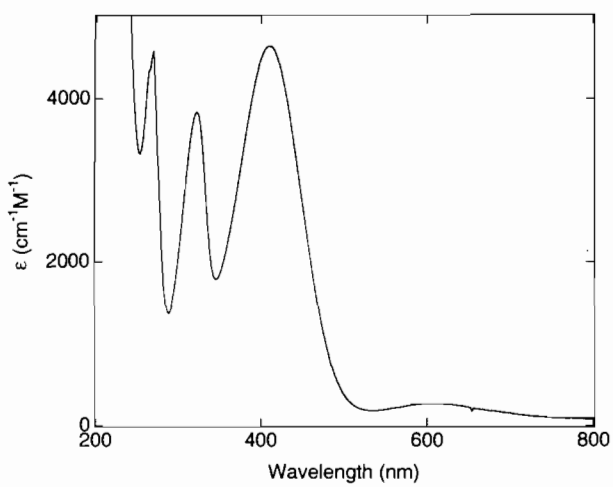

Fig. 5. UV–Vis spectrum of $[CuH_8TAAB](ClO_4)_2$ in water.

for the nickel complex [11,21]. The UV–Vis spectra of the copper complex of H_8TAAB in water is shown in Fig. 5. The absorption maxima are at wavelengths (nm (ϵ, cm^{-1} M^{-1})): 268 (4650), 322 (3900), 408 (4650), 614 (245).

3.4. Electrochemistry

The cyclic voltammogram and the differential pulse voltammetry of the CuH_8TAAB complex are shown in Fig. 6. Two cathodic processes are observed and a very sharp anodic peak which is due to anodic stripping of the copper metal electrodeposited on the electrode [22]. The peak potential in differential pulse voltam-

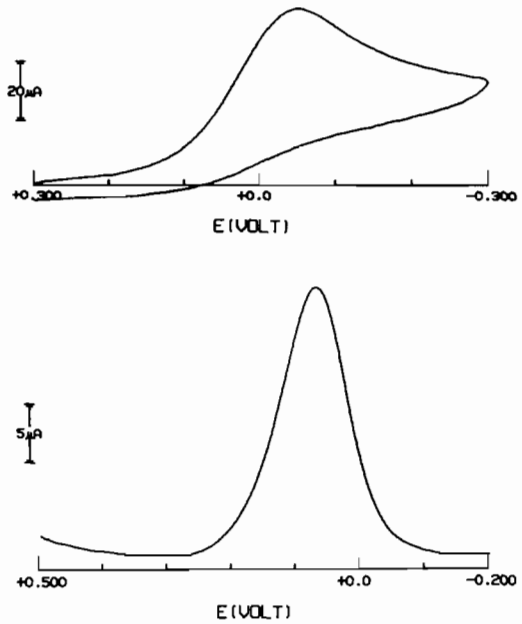

Fig. 6 (a) Cyclic voltammogram of $[CuH_8TAAB](ClO_4)_2$ in acetonitrile–0.1 M tetrapropylammonium perchlorate measured with a glassy carbon electrode vs. SCE at a sweep rate of 0.1 V s^{-1} (22 °C). (b) Differential pulse voltammogram of $[CuH_8TAAB](ClO_4)_2$ with a pulse height of 50 mV and a scan rate of 4 mV s^{-1}.

metry was at +72 mV versus SCE and −320 mV versus ferrocene.

4. Discussion

Busch and co-workers first obtained the nickel complex of H_8TAAB by reducing the nickel complex of TAAB with hydrogen on a platinum catalyst [11] and secondly by reaction of nickel(II) with H_8TAAB [4,21]. The hydrogenation of the copper(II) complex of TAAB did not lead to the copper(II) complex of H_8TAAB but instead the copper(I) complex of TAAB was obtained [11]. The same complex was obtained using ascorbic acid for the reduction [23]. The reaction of H_8TAAB with copper(II) was not reported and we used this method to obtain the copper(II) complex of H_8TAAB. As described in Section 2, it is also possible to obtain this complex by reduction of the copper(II) complex of TAAB with sodium borohydride. While the direct reduction of the acid salts of the self condensation products of *o*-aminobenzaldehyde with sodium borohydride led to the product H_4TAAB which was reduced to H_8TAAB with $LiAlH_4$ [4,21], the reduction of the copper complex of TAAB led right away to the fully saturated macrocyclic complex. The nickel complex was extensively described by Busch and co-workers [11] with the exception of the structure of this complex and is not further discussed here.

The UV–Vis spectrum of the copper(II) complex of H_8TAAB has absorption maxima at 268 and 322 nm that we assign as intraligand bands, while the absorption maxima at 408 nm is ascribed to a ligand to metal charge transfer band (LMCT) from the tertiary amine N to Cu(II) [24]. The lowest energy band at 618 nm is assigned as a ligand field transition of the copper(II) center. That no imine bonds are present in this complex was confirmed by IR spectroscopy, where the –C=N– stretching modes were missing as was found for the nickel complex [11,21]. The electrochemistry of the copper complex of H_8TAAB showed that the reduction process was not electrochemically reversible. This is in contrast to the copper complex of TAAB for which quasi-Nernstian behavior was observed [8]. This is understandable because copper(I) is more stabilized by imino nitrogen donors than by the amino nitrogen donors.

Amino bonds are easily oxidized to imino bonds and because of our interest in working with low valent metal ions we tried to avoid this problem by a complete methylation of the nitrogen atoms. Unfortunately it has been so far impossible to synthesize metal complexes of the macrocycle Me_4H_4TAAB. The reason for that we assume is the rigid steric structure forced onto the macrocycle through the methylation.

In comparing the four structures one can observe the effect metal coordination has on the bond lengths in a macrocycle. The greatest change in bond length in this macrocyclic ligand due to metal coordination can be observed in the bond lengths involving the nitrogen atoms of the macrocycle. These bond lengths are listed in Table 7. The average N–C(methylene) bond length is 1.445(9) Å in the free ligand **I** and 1.496(12) Å in the metallated macrocycles **II** and **III** with an intermediate value of 1.465(7) Å in the methylated ligand **IV**. The same trend can be seen in the average value of the N–C(ring) bond length which increases from 1.398(9) Å in the free ligand to 1.451(16) Å in the coordinated macrocycle with an intermediate value of 1.432(20) in the methylated ligand. In the free ligand **I** as well as in the coordinated ligands **II** and **III** the four nitrogen atoms are approximately coplanar. When the amine hydrogens are replaced by larger methyl groups as is found in **IV**, the steric repulsion caused by these larger methyl groups causes the ligand to twist to relieve this strain so that the nitrogen atoms are no longer coplanar as is observed in **IV**.

A comparison of the structure of the H_8TAAB complex of Ni^{2+} and Cu^{2+} with the structures of the TAAB complex of Ni^{2+} and the MeTAAB [25] complex of Cu^{2+} shows that in all these cases the ligand retains the saddle shape, with adjacent benzene rings tilted towards opposite sides of the plane of the macrocycle. Both nickel(II) complexes are high spin with the Ni–N bond lengths being 0.045 Å longer with the reduced ligand. The copper complexes are more difficult to compare because with MeTAAB the complex is a

bicapped square pyramid with two oxygen atoms of a nitrate ion coordinated in the axial position. The equatorial bonds are 0.114 Å longer with the reduced ligand but the axial bonds are 0.20 Å shorter.

In comparing the structures of the 16-membered macrocycles H_8TAAB and Me_4H_4TAAB with the structure of the 14-membered macrocycle 1,4,8,11-tetramethyl-1,4,8,11-tetraazadibenzo[*b*,*i*]cyclotetradecane (TMBC) [14] we can see that in the copper complex of TMBC the four methyl groups are all on the same side of the macrocycle while in the copper complex of H_8TAAB, the hydrogen atoms adjacent to one another are on opposite sides of the macrocycle. In TMBC metal complexes the benzene rings are both on the side of the macrocycle opposite the methyl groups whereas with H_8TAAB the hydrogen atoms *trans* to one another are on the same side of the macrocycle. In the free ligand of TMBC the four nitrogen atoms are within ± 0.08 Å of the plane defined by these four nitrogen atoms whereas in Me_4H_4TAAB the nitrogen atoms are severely distorted from planarity to avoid contacts between the methyl groups and the benzene rings. Steric interactions between the methyl groups and the benzene rings of the macrocycle because of the preferred saddle shape of the ligand are probably responsible for the difficulty in obtaining metal complexes with this ligand.

Complexes of the reduced form of the tridentate condensation product of *o*-aminobenzaldehyde TRI are not known so far. The macrocycles with methylated or benzylated nitrogens were synthesized by Ollis and coworkers [26]. The methylated form is reported as unstable. Our attempts to reduce the macrocycle bound to Ni(II) similar to our work on the reductions on the TAAB complexes were unsuccessful.

5. Supplementary material

Tables of crystallographic data collection parameters, anisotropic thermal parameters for non-hydrogen atoms, hydrogen atom positional and thermal parameters, complete listing of bond length and angles, table of hydrogen bonding schemes and listing of structure factors are available from D.J.S. on request.

Acknowledgements

We thank Dr Carol Creutz and Dr E. Fujita for helpful discussions. This research was carried out at Brookhaven National Laboratory under contract DE-AC02-76CH00016 with the US Department of Energy and supported by its Division of Chemical Sciences, Office of Basic Energy Sciences.

References

[1] E. Fujita, C. Creutz, N. Sutin and D. Szalda, *J. Am. Chem. Soc., 113* (1991) 343.
[2] G.A. Melson and D. H. Busch, *J. Am. Chem. Soc., 87* (1965) 1706.
[3] G.A. Melson and D.H. Busch, *J. Am. Chem. Soc., 86* (1964) 4834.
[4] J.S. Skuratowicz, I.L. Madden and D.H. Busch, *Inorg. Chem., 16* (1977) 1721.
[5] S.C. Cummings and D.H. Busch, *J. Am. Chem. Soc., 92* (1970) 1924.
[6] S.C. Cummings and D.H. Busch, *Inorg. Chem., 10* (1971) 1220.
[7] G.A. Melson and D.H. Busch, *J. Am. Chem. Soc., 86* (1964) 4830.
[8] N. Takvoryan, K. Farmery, V. Katovic, F.V. Lovecchio, E.S. Gore, L.B. Anderson and D.H. Busch, *J. Am. Chem. Soc., 96* (1974) 731.
[9] L.T. Taylor, S.C. Vergaz and D.H. Busch, *J. Am. Chem. Soc., 88* (1966) 3170.
[10] L.T. Taylor and D.H. Busch, *Inorg. Chem., 8* (1969) 1366.
[11] V. Katovic, L.T. Taylor, F.L. Urbach, W.H. White and D.H. Busch, *Inorg. Chem., 11* (1972) 479.
[12] V. Katovic, S.C. Vergaz and D.H. Busch, *Inorg.Chem., 16* (1977) 1716.
[13] C.L. Lane, *Synthesis,* (1975) 135.
[14] D.-D. Klaehn, H. Paulus, R. Grewe and H. Elias, *Inorg. Chem., 23* (1984) 483.
[15] *International Tables for X-ray Crystallography,* Vol. I, Kynoch, Birmingham, UK, 1969, (a) p. 99; (b) p. 75.
[16] R.E. Marsh, *Inorg. Chem., 27* (1988) 2902 (see appendix by G. Williams).
[17] G.M. Sheldrick, *SHELX 76,* crystal structure refinement program, Cambridge University, UK, 1976.
[18] Neutral-atom scattering factors: *International Tables for X-ray Crystallography,* Vol. IV, Kynoch, Birmingham, UK, 1974, p. 99–100; Anomalous dispersion factors: D.T. Cromer and D. Weinmann, *J. Chem. Phys., 53* (1970) 1891.
[19] T. Ito and K. Toriumi, *Acta Crystallogr., Sect. B, 37* (1981) 240.
[20] T. Ito, K. Toriumi, *Acta Crystallogr., Sect. B, 37* (1981) 88.
[21] J.S. Skuratowicz, Synthesis and characterization of some complexes containing macrocyclic ligands derived from *o*-aminobenzaldehyde, *Thesis*, The Ohio State University, USA, 1973.
[23] A. Cinquantini, G. Opromolla and P. Zanello, *J. Chem. Soc., Dalton Trans.,* (1991) 3161.
[23] E.J. Pulliam and D.R. McMillin, *Inorg. Chem., 23* (1983) 1172.
[24] S. Schindler, D.J. Szalda and C. Creutz, *Inorg. Chem., 31* (1992) 2255.
[25] A.J. Jircitano, R.I. Sheldon and K.B. Mertes, *J. Am. Chem. Soc., 105* (1983) 3022.
[26] A. Hoorfar, W.D. Ollis, J.A. Price, S.J. Stephanatou and J.F. Stoddart, *J. Chem. Soc., Perkin Trans.,* (1982) 1649.